

Simulation of Finite Width Effects in Physics Beyond the Standard Model

M.A. Gigg

IPPP, Department of Physics, Durham University
Email: m.a.gigg@durham.ac.uk

P. Richardson,

IPPP, Department of Physics, Durham University; and
Physics Department, CERN
Email: peter.richardson@durham.ac.uk

ABSTRACT: We present a method for the inclusion of finite width effects in the simulation of Beyond Standard Model (BSM) physics. In order to test the validity of the method we compare our results with matrix elements for a range of production and decay processes in the Standard Model, Minimal Supersymmetric Standard Model (MSSM) and Minimal Universal Extra Dimensions model (MUED). This procedure has been implemented in the Herwig++ event generator and will be available in a forthcoming release.

KEYWORDS: Beyond Standard Model – Standard Model – Hadronic Colliders – Phenomenological Models – Supersymmetric Standard Model.

Contents

1. Introduction	1
2. Narrow Width Approximation	2
3. Off-Shell Weight Factor	3
3.1 Off-shell Masses in Particle Production	4
3.2 Off-Shell Effects in Particle Decay	7
4. Examples	8
4.1 Decay via an Off-Shell Fermion	9
4.2 Decay via an Off-Shell Gauge Boson	9
5. Off-Shell Cross Sections	10
6. Merging Two- and Three-Body Decays	11
7. Summary	13
A. Derivation of Weight Factor	14

1. Introduction

It has been believed for some time that there must be new physics at the TeV scale. While most theories of physics beyond the Standard Model differ in their internal workings they all possess a common feature, the appearance of a spectrum of heavy states that will be produced at a collider with sufficient energy. If there is to be any hope of discovering these new particles one must have accurate simulations of the signals they will produce, and in particular, accurate simulations that can be compared directly with experimental data. There are, essentially, two methods of producing events distributed as they would be in an experiment. The first is to use a matrix element generator [1–6] to compute the full $2 \rightarrow n$ matrix element for a specific final state of interest, including the decays of all of the fundamental particles. This can then be interfaced to a general-purpose event generator to produce the particles observed in an experiment. The advantages are that the full matrix element calculation gives contributions from non-resonant diagrams which may be important and the effects of spin correlations are automatically included. Ideally, we would use an n -body matrix element for all processes, however, there are a number of issues:

1. the time to compute the full matrix element, even if only the resonant diagrams are included, grows with the number of final-state particles. This is particularly problematic for models such as supersymmetry which can contain long decay chains;
2. many new physics models introduce a large number of new states, which lead to many possible production and decay mechanisms. If the full calculation is used in all cases the number of processes required becomes prohibitively large;
3. any new coloured states will emit QCD radiation in their production and decay which must be simulated using the parton shower approximation.

Given these issues, for the foreseeable future, we will need to use general purpose event generators [7–12] that treat the production and decay of heavy particles in a factorised approximation. If a generator incorporates the model of interest it can simulate everything from the initial hard interaction up to the final colour-singlet particles that interact with a detector. The production step is typically a simple $2 \rightarrow 2$ scattering followed by a series of perturbative decays which result in stable particles that are hadronized and decayed to give the observed colour-singlet states¹. It is vital that these simulations are as accurate as possible by, for instance, including effects such as spin correlations [13–15] throughout the event simulation.

Another area where the factorized approach can neglect important physics is in the treatment of off-shell effects, as by definition the method must use the narrow width approximation to separate production and decay. In the simplest approach all particles are on-shell throughout their production and decay [16], which in many scenarios is a good enough approximation but in other regimes, *e.g.* close to thresholds and for resonances, such as the Z^0 boson, where the width can be measured, this approach is unsatisfactory. In order to improve the physics of the simulation, off-shell effects must be included in the production and decay stages of the event generation. The aim of this paper is to describe how this can be achieved and discuss its implementation in the Herwig++ event generator [7].

The next section describes the narrow width approximation in more detail, Sect. 3 gives a description of the method by which we include width effects, with specific examples for the production and decay stages. Section 4 gives results for various scenarios in the Minimal Supersymmetric Standard Model (MSSM) and the Minimal Universal Extra Dimensions (MUED) model, some conclusions are drawn in the final section.

2. Narrow Width Approximation

In general the evaluation of the matrix element for a process with a high multiplicity final state is complex due to the factorial growth in the number of diagrams. The calculation can be simplified by using the narrow width approximation, where if:

1. the resonance has a small width Γ compared with its pole mass M , $\Gamma \ll M$;

¹This is an extremely simplified schematic of event generation. More detail can be found in, for example, Ref. [7].

2. we are far from threshold, $\sqrt{s} - M \gg \Gamma$, where \sqrt{s} denotes the centre-of-mass energy;
3. the propagator is separable;
4. the mass of the parent is much greater than the mass of the decay products;
5. there are no significant non-resonant contributions;

the cross section integral can be separated into an on-shell production step followed by a series of decays. The separation arises from integrating out the propagators connecting each step giving a momentum independent factor

$$\int_{-\infty}^{\infty} dq^2 \left| \frac{1}{(q^2 - M^2) + iM\Gamma} \right|^2 = \frac{\pi}{M\Gamma}. \quad (2.1)$$

If the above assumptions are true one obtains an estimate of the cross section with an error of $O(\Gamma/M)$ using this approach.

In reality, especially when dealing with BSM physics, the approximation is commonly used when the above assumptions are not strictly satisfied. While there have recently been studies of the validity of narrow width limit for some SUSY scenarios [17–19], nothing has been studied in relation to other popular new physics models. In the next section we describe how off-shell effects can be simulated with our main focus on BSM studies. In `Herwig++` the same approach is used for the simulation of off-shell effects in hadron decays, allowing the same infrastructure to handle all decays.

3. Off-Shell Weight Factor

As discussed above, the narrow width approximation allows the propagator connecting production and decay of successive decays to be integrated out. This essentially means that part of the phase-space integral is approximated to a constant when the correct assumptions are satisfied. Therefore, to improve the accuracy of our simulation we wish to move away from the on-shell approximation and include the effects from integrating over the connecting propagator. In the past this has been accomplished in a variety of ways. For example, the FORTRAN HERWIG [8] program included:

1. the full three-body matrix element, with an off-shell W^\pm boson, for top decay;
2. smearing of fundamental particle masses using a Breit-Wigner distribution;
3. a more sophisticated Higgs boson lineshape [20].

To improve our simulation we include the weight factor (see Sect. A for a derivation)

$$\frac{1}{\pi} \int_{m_{\min}^2}^{m_{\max}^2} dm^2 \frac{m\Gamma(m)}{(m^2 - M^2)^2 + m^2\Gamma^2(m)}, \quad (3.1)$$

throughout the production and decay stages, where $\Gamma(m)$ is the running width of the particle, M is the pole mass and $m_{\min, \max}$ are defined such that the maximum deviation

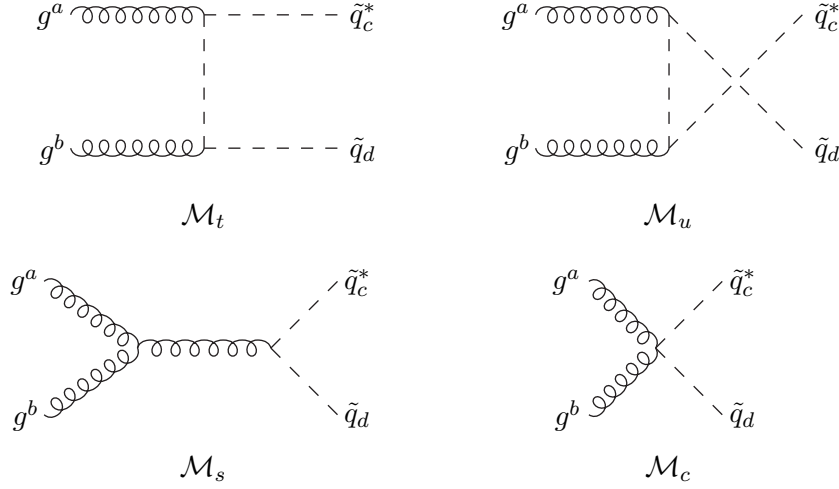


Figure 1: Feynman diagrams for the process $gg \rightarrow \tilde{q}^* \tilde{q}$ where the Roman indices give the colour representation.

from the pole mass is a constant times the on-shell width. The weight includes a momentum dependence into the calculation of cross sections and decay widths thereby improving the approximation to the full matrix element. While for the latter case convoluting the weight with the partial width calculation for a particular decay mode is relatively simple, this is not the case for the production stage, so we will consider them separately.

3.1 Off-shell Masses in Particle Production

For production we need to convolute the weight factor described above with the cross section integral. We achieve this by distributing the masses of the outgoing particles according to Eq. (3.1). This in itself is a trivial task but what we will show here, with an example from supersymmetry, is that gauge invariance can be violated if these masses are used naïvely when calculating the matrix elements.

Consider the process $gg \rightarrow \tilde{q}^* \tilde{q}$, for which the diagrams are shown in Fig. 1, where we wish the outgoing squarks to have masses m_3 and m_4 respectively. Due to the presence of external gluons, the Ward identity

$$p_{1\mu} p_{2\nu} \mathcal{M}^{\mu\nu}(p_1, p_2) = 0 \quad (3.2)$$

where p_i are the momenta of the gluons and \mathcal{M} is the total amplitude, must be satisfied.

After replacing the external polarization vectors with their momenta the amplitudes are given by

$$\mathcal{M}_t = -g_s^2 \frac{(t - m_3^2)}{(t - m_t^2)} (m_4^2 - t) t_{di}^b t_{ic}^a, \quad (3.3a)$$

$$\mathcal{M}_u = -g_s^2 \frac{(u - m_4^2)}{(u - m_u^2)} (m_3^2 - u) t_{di}^a t_{ic}^b, \quad (3.3b)$$

$$\mathcal{M}_s = -\frac{g_s^2}{2} (t - u) \left(t_{di}^b t_{ic}^a - t_{di}^a t_{ic}^b \right), \quad (3.3c)$$

$$\mathcal{M}_c = \frac{g_s^2}{2} s \left(t_{di}^a t_{ic}^b + t_{di}^b t_{ic}^a \right), \quad (3.3d)$$

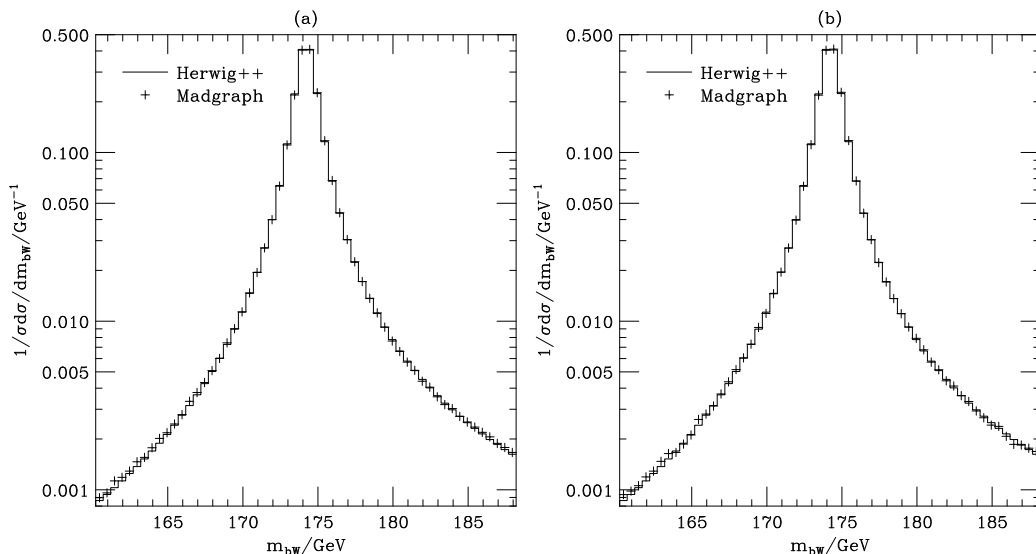


Figure 2: The top quark line shape for $m_t^{\text{pole}} = 174.20$ GeV and $\Gamma_t(m_t^{\text{pole}}) = 1.40$ GeV at the ILC with the results of **Herwig++** for $e^+e^- \rightarrow t\bar{t} \rightarrow b\bar{b}W^+W^-$ compared to the Madgraph calculation of $e^+e^- \rightarrow b\bar{b}W^+W^-$ with the Madgraph result including (a) all diagrams containing a top quark line and (b) all diagrams excluding those containing a Higgs boson. In both cases the **Herwig++** result uses our off-shell treatment while the Madgraph result includes all diagrams for the $2 \rightarrow 4$ scattering process, including the non-resonant contribution.

where s , t and u are the Mandelstam variables, $m_{t,u}$ are the t - and u -channel masses and t_{ij}^a are the SU(3) colour matrices. Equations (3.3a) and (3.3b) show that for any hope of achieving the correct cancellation we must set $m_t = m_3$ and $m_u = m_4$. This also shows why, even in the on-shell case, one must take care when using widths in scattering diagram calculations as these alone can give rise to violations of gauge invariance. The total amplitude saturated with the gluon momenta for the $g g \rightarrow \tilde{q}^* \tilde{q}$ process is then

$$\frac{g_s^2}{2} (m_3^2 - m_4^2) [t^b, t^a], \quad (3.4)$$

so that Eq. (3.2) is only satisfied if $m_3 = m_4$.

This requirement means that, in general, we cannot use off-shell masses when calculating matrix elements since if we generate a process such as that shown, we would violate gauge invariance. In our procedure the off-shell masses are used when calculating the momenta of the outgoing particles involved in the hard interaction but are then rescaled, such that $m_3 = m_4$, for the matrix element calculations. To demonstrate the validity of this procedure we compare the line shape of the top quark from **Herwig++** and Madgraph for the production of a top quark at the ILC, the Tevatron and the LHC. In **Herwig++** the top quark width is computed using the full three-body matrix element whereas in the Madgraph case just the two-body decay of the top quark is used, due to rapid growth in the number of diagrams that are required. In all cases **Herwig++** generates the $2 \rightarrow 2$ production process for the $t\bar{t}$ pair followed by the three-body decay of the top quark using the treatment of off-shell effects described in the text. Madgraph was used to calculate

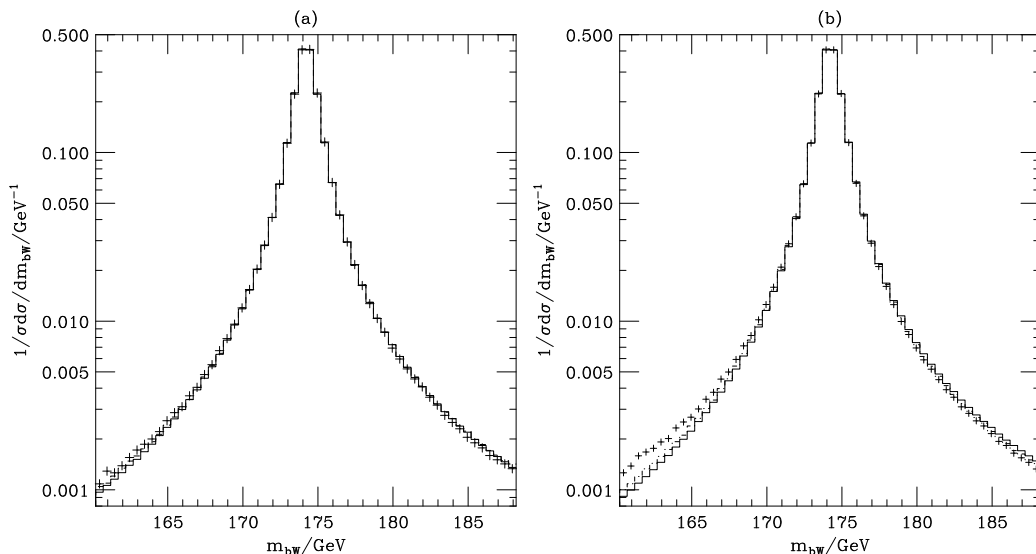


Figure 3: The top quark line shape for $m_t^{\text{pole}} = 174.2 \text{ GeV}$ and $\Gamma_t(m_t^{\text{pole}}) = 1.4 \text{ GeV}$ at (a) the Tevatron and (b) the LHC. The black line denotes the results from `Herwig++` with the outgoing masses rescaled to their on-shell value, the dot-dash line denotes `Herwig++` with the outgoing masses rescaled to their average value and the crosses denote the Madgraph results. The `Herwig++` results were generated using the $2 \rightarrow 2$ production process for $t\bar{t}$ followed by the three-body decay of the top quarks. The Madgraph results use the full matrix element for the production of $b\bar{b}W^+W^-$ to order $\alpha_S^2\alpha_W^2$, including all diagrams, both resonant and non-resonant diagrams, containing a top quark line.

the $2 \rightarrow 4$ matrix element for the production of $b\bar{b}W^-W^+$ including the non-resonant diagrams.

To ensure that the amplitudes generated by Madgraph [1] were gauge invariant, the “fudge-factor” scheme [21] was used. This involves calculating the full amplitude without the inclusion of the width for any off-shell propagators and then multiplying the full amplitude, including non-resonant contributions, by

$$\frac{p^2 - M^2}{p^2 - M^2 + iM\Gamma} \quad (3.5)$$

for any propagator that can be on-shell, *i.e.* for which it is possible for $p^2 = M^2$ within the physically allowed phase space. This is the simplest approach that ensures the amplitude is gauge invariant [21], although it has the drawback that the non-resonant diagrams are affected. A more detailed discussion of the issue of gauge-invariance when including non-resonant diagrams can be found in [21].

For the ILC case, Fig. 2, the Madgraph result is shown for both the process including only the diagrams with a top quark line and also the process including all electroweak diagrams, resonant and non-resonant, excluding the Higgs. There is excellent agreement between our results and those performed with the full matrix element giving us confidence in our procedure. For the hadron colliders we must consider the rescaling since there will be processes such as $gg \rightarrow t\bar{t}$ that will, as discussed above, violate gauge invariance when we

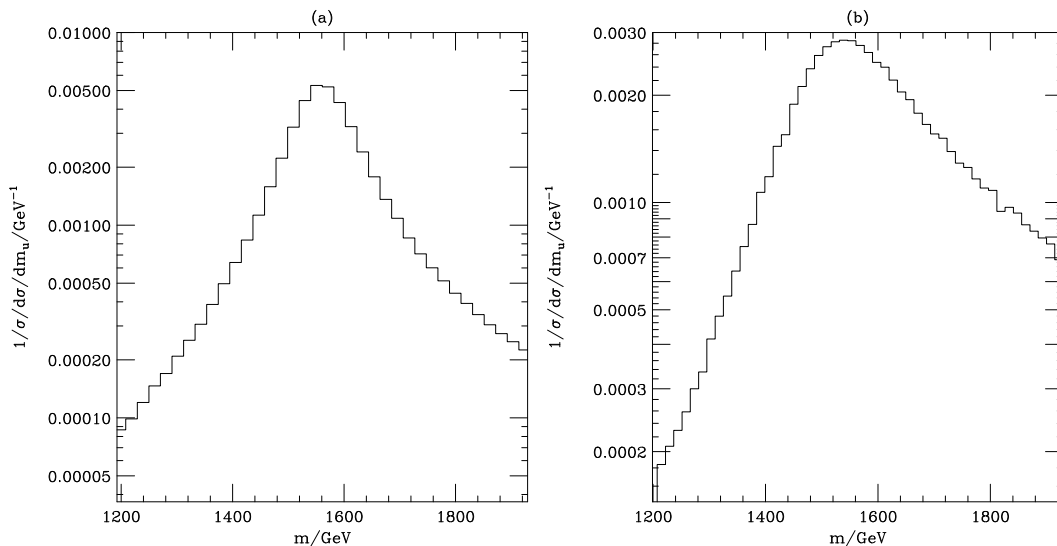


Figure 4: The line shapes for (a) the SUSY partner to the u -type doublet field and (b) the level-1 KK partner to the u -type doublet field.

take the top quark off-shell. Here we will compare two choices for the momenta rescaling, first rescaling such that the masses have their on-shell value and second rescaling to the average value of the outgoing masses $(m_3 + m_4)/2$. The results for the Tevatron and the LHC are shown in Fig. 3. The Tevatron results are in excellent agreement with the matrix element for both choices of rescaling and the LHC is good agreement except for the tail where there is a small deviation. It is clear that either choice for the value of the rescaled mass gives good agreement with the matrix element but in the LHC case choosing to rescale to the average value of the outgoing masses gives slightly better agreement with the full calculation.

Figure 4 shows the mass distributions for a left-handed up squark in the MSSM² and the KK-partner of the doublet quark in the MUED model respectively. The mass spectrum for the MUED case is matched to the SUSY spectrum at SPS point 2 [22] where $m_{\tilde{u}_L} = 1560.97$ GeV, $\Gamma_{MSSM} = 70.22$ GeV and $\Gamma_{MUED} = 312.76$ GeV.

This example is at the extreme of where this method should be applied since, especially in the MUED case, the width is large and in general there could be sizeable non-resonant contributions.

3.2 Off-Shell Effects in Particle Decay

Many new physics models have spectra that result in long chains between the production of a resonance and a stable state. As mentioned previously the simplest approach in dealing with these chains is via a series of on-shell cascade decays. While this may be an appropriate approximation in some kinematic regions, in others, *i.e.* when the decaying

²It is technically incorrect to say that a scalar particle has a helicity state but the terminology allows for easier distinction between the partners of the SU(2) doublet and singlet quarks.

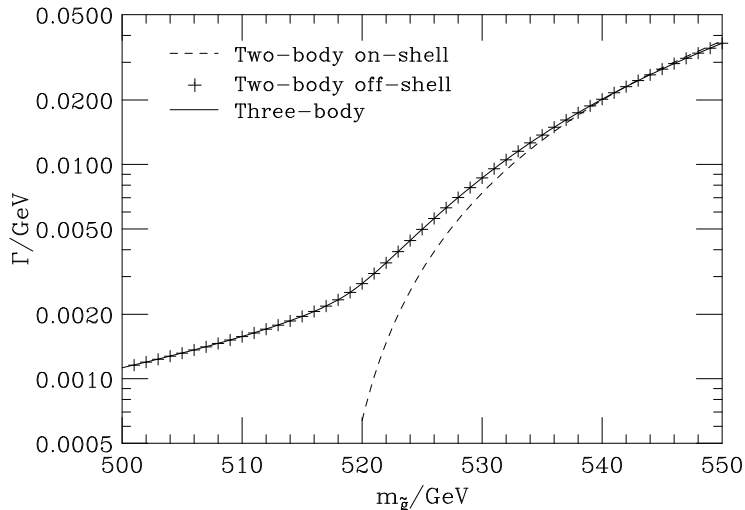


Figure 5: The partial width for the decay mode $\tilde{g} \rightarrow \bar{b}\tilde{b}_1 \rightarrow \tilde{\chi}_2^0 b$ in the MSSM.

particle is close to threshold, the effects from the off-shell propagator must be taken into account.

This can be achieved by including the weight factor from Eq. (3.1) in the calculation of the partial width of a selected decay mode. For example, consider the decay $\tilde{g} \rightarrow \bar{b}\tilde{b}_1 \rightarrow \tilde{\chi}_2^0 b\bar{b}$, the partial width is

$$\Gamma(\tilde{g} \rightarrow \tilde{\chi}_2^0 b\bar{b}) = \frac{1}{\pi} \int_{m_{\min}^2}^{m_{\max}^2} dm^2 \frac{m\Gamma(\tilde{b}_1 \rightarrow \tilde{\chi}_2^0 b)}{(m^2 - M^2)^2 + M^2\Gamma(m)^2} \Gamma(\tilde{g} \rightarrow \bar{b}\tilde{b}_1), \quad (3.6)$$

where the widths inside the integral are evaluated for the off-shell mass m . The limits on the integration are determined by the on-shell width and are set such that the maximum deviation from the pole mass of \tilde{b}_1 is 5Γ . As the intermediate particle is a scalar, the inclusion of the weight factor should give exact agreement with the full three-body calculation providing the integral is performed over the same phase space. Fig 5 demonstrates this for SPS point 1a where the three-body phase-space is restricted to the same as the two-body case. The spectrum was produced using `SPheno 2.2.3` [23] where $m_{\tilde{b}_1} = 515.27$ GeV, $\Gamma(m_{\tilde{b}_1}) = 3.83$ GeV and $m_{\tilde{\chi}_2^0} = 180.58$ GeV. The mass of the b -quark is $m_b = 4.20$ GeV, which is the default value in `Herwig++`. The on-shell result is also included for reference.

The agreement between the full matrix element calculation and our results show that the approximation is valid.

4. Examples

Here we present a range of processes in the MSSM and the MUED model demonstrating the consistency of the inclusion of off-shell effects in `Herwig++`. In the decay examples the comparison is always to the full three-body result, which was included in `Herwig++` as a modification to the current released version and will be included in a future version along with the simulation of finite width effects.

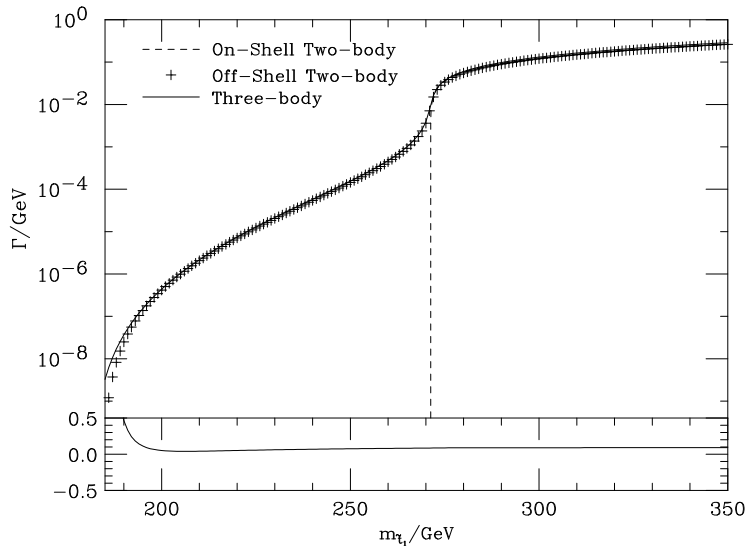


Figure 6: The partial width for the decay mode $\tilde{t}_1 \rightarrow \tilde{\chi}_1^0 t \rightarrow W^+ b \tilde{\chi}_1^0$. The lower panel gives the value of $(\Gamma_{\text{three}}/\Gamma_{\text{off}} - 1)$.

4.1 Decay via an Off-Shell Fermion

A possible two-body decay of the \tilde{t}_1 squark in the MSSM is $\tilde{t}_1 \rightarrow \tilde{\chi}_1^0 t$. If $m_{\tilde{t}_1} \approx m_{\tilde{\chi}_1^0} + m_t$ then the effect of the width of the top quark must be considered. We choose the decay mode $\tilde{t}_1 \rightarrow \tilde{\chi}_1^0 t \rightarrow \tilde{\chi}_1^0 W^+ b$ at SPS point 1a [22] where $m_{\tilde{\chi}_1^0} = 97.04$ GeV with $m_t = 174.20$ GeV, $m_W = 80.40$ GeV and $m_b = 4.20$ GeV. The threshold values for the on-shell two- and three-body decays of the \tilde{t}_1 are 271.24 GeV and 181.64 GeV respectively. Figure 6 shows partial width of the \tilde{t}_1 as a function of its mass for the three-body, two-body off-shell and two-body on-shell results.

Unlike the gluino decay example in Sect. 3.2 the W^\pm boson, like the top quark, has a measured decay width and this should be treated properly. In the example shown in Fig. 6 the running width for the top quark is calculated from its full three-body matrix element to a b -quark and a pair of light fermions which includes the full effects of the W^\pm width. The agreement between the two-body off-shell and three-body results shows that this is a valid approximation to use. Also, despite the extra factor of $(\not{p} + m)$ in the numerator of the fermion propagator, there is still good agreement between the full three-body result and the two-body result with weight factor even though the factor does not attempt to include this. This is due to the numerator factor being largely responsible for propagating spin information rather than altering the kinematics.

4.2 Decay via an Off-Shell Gauge Boson

In the MSSM there is a coupling between the Z^0 boson and the gaugino sector allowing for a three-body decay of the second neutralino to a pair of light fermions via an intermediate Z^0 boson. The presence of a spin-1 rather than a spin-0 particle alters the form of the partial width as the decay is now p -wave and not s -wave, as in Fig. 5. To illustrate that the weight

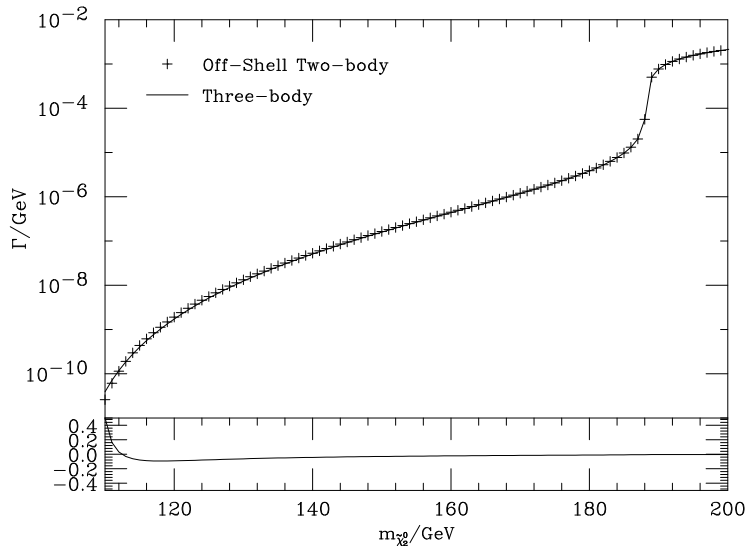


Figure 7: The partial width for $\tilde{\chi}_2^0 \rightarrow \tilde{\chi}_1^0 Z^0 \rightarrow b\bar{b}\tilde{\chi}_1^0$ in the MSSM. The lower panel gives the value of $(\Gamma_{\text{three}}/\Gamma_{\text{off}} - 1)$.

formula works just as well in this situation we choose the decay chain $\tilde{\chi}_2^0 \rightarrow \tilde{\chi}_1^0 Z^0 \rightarrow \tilde{\chi}_1^0 b\bar{b}$ at SPS point 1a where $m_{\tilde{\chi}_1^0} = 97.04$ GeV with $M_Z = 91.19$ GeV and $m_b = 4.20$ GeV.

Figure 7 shows the results for the above decay and demonstrates that there is good agreement between the full three-body result and the two-body approximation for an intermediate vector particle. Another example of a possible p -wave decay is $u^\bullet \rightarrow u e_1^{\circ-} e^+$ in the MUED model where the intermediate particle is the level-1 KK- Z^0 boson. For parameter values $R^{-1} = 500$ GeV and $\Lambda R = 20$ the relevant masses are $M_{Z_1^0} = 535.81$ GeV and $M_{e_1^{\circ-}} = 504.25$ GeV. The partial width is shown in Fig. 8, again with both the three-body result and two-body via an off-shell Z_1^0 .

5. Off-Shell Cross Sections

In the narrow width approximation, the cross section for a particular final state is computed by taking the on-shell production cross section to an intermediate resonance and multiplying by the branching fraction to the final state of interest. If the on-shell mass of the resonance is close the threshold for the decay into the final state then the narrow width approximation is invalid and one should calculate the full matrix element. As described in Sect. 3 and demonstrated in Sect. 4 we can include a weight factor in production and decay to simulate off-shell behaviour. In the case of calculating cross sections for specific processes, this amounts to including the effect of propagator widths in the Monte Carlo estimate of such a quantity. It is important to note, however, that a general purpose event generator that starts from a $2 \rightarrow 2$ hard scattering and then perturbatively decays the produced resonances can never include non-resonant contributions. This is a fundamental limit of the approximations used to generate the events. Nevertheless, a good approximation

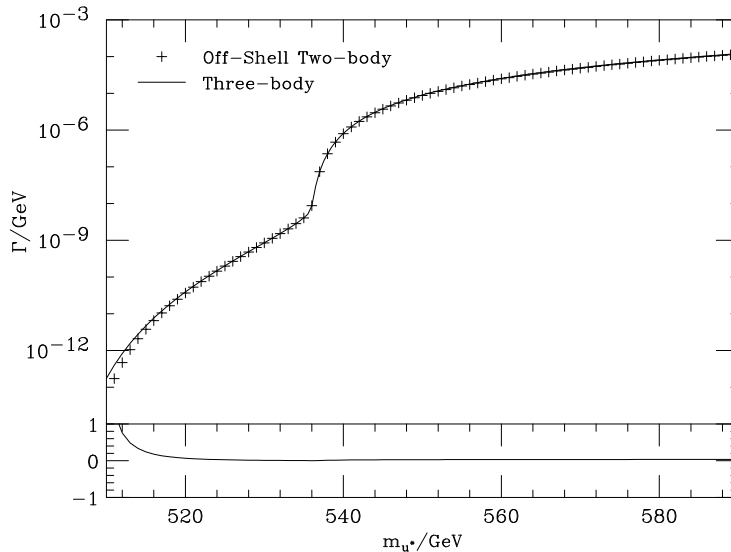


Figure 8: The partial width for $u^\bullet \rightarrow u e_1^{\circ-} e^+$ in the MUED model. The lower panel gives the value of $(\Gamma_{\text{three}}/\Gamma_{\text{off}} - 1)$.

can still be achieved providing one uses the simulations with care³.

An example of a process that has no non-resonant contributions is the production of a strange squark via $u \bar{d} \rightarrow \tilde{\chi}_1^+ \tilde{g} \rightarrow \tilde{\chi}_1^+ \tilde{s}_L \bar{s}$, the diagrams for which are shown in Fig. 9. The results for the ratio of the off-shell to the on-shell cross section as a function of the strange squark mass are shown in Fig. 10 for SPS point 1a. The ratio is constant, with the off-shell result smaller due to the integration limits no longer being taken to infinity, until $m_{\tilde{s}_L} \approx 0.8m_{\tilde{g}}$ where we are in the threshold region for the decay of the gluino. The sudden steep rise as the mass ratio approaches unity is due to the on-shell cross section going to zero at threshold.

There is a counterpart process to that in Fig. 9 for MUED, where the $\tilde{\chi}_1^+$ is replaced by the W_1^+ boson, the \tilde{g} by the g_1 and \tilde{s}_L by the s_1^\bullet . The ratio of the on-shell to the off-shell cross section for this process is also shown in Fig. 10 where the masses for the MUED particles have been matched to SUSY spectrum to give a fair comparison. It is apparent here that the spins of the underlying model play only a small role in determining the value of this ratio as the results are similar while the absolute values of the cross sections may differ greatly, taking the colour octet object off-shell affects only the kinematics.

6. Merging Two- and Three-Body Decays

In Sect. 4 we demonstrated the accuracy of including an off-shell weight factor by comparison with the full three-body matrix element for a variety of processes. For each process considered the width was plotted over the entire kinematic range, rather than restricting to the region where the decay would be applicable, to give a full comparison. In a real

³In some specific cases non-resonant effects can be modelled by using a modified form of Eq. (3.1), for example the Higgs lineshape [20].

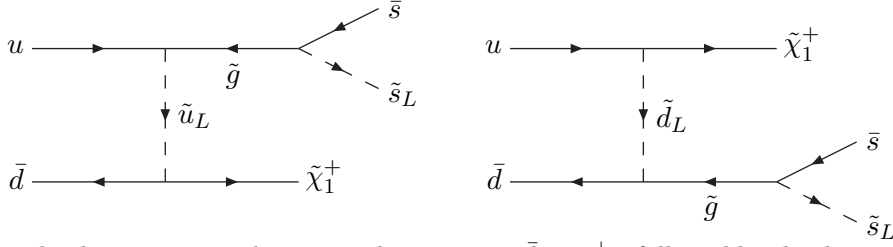


Figure 9: The diagrams contributing to the process $u \bar{d} \rightarrow \tilde{\chi}_1^+ \tilde{g}$ followed by the decay of the gluino to a strange quark and a left-handed strange squark.

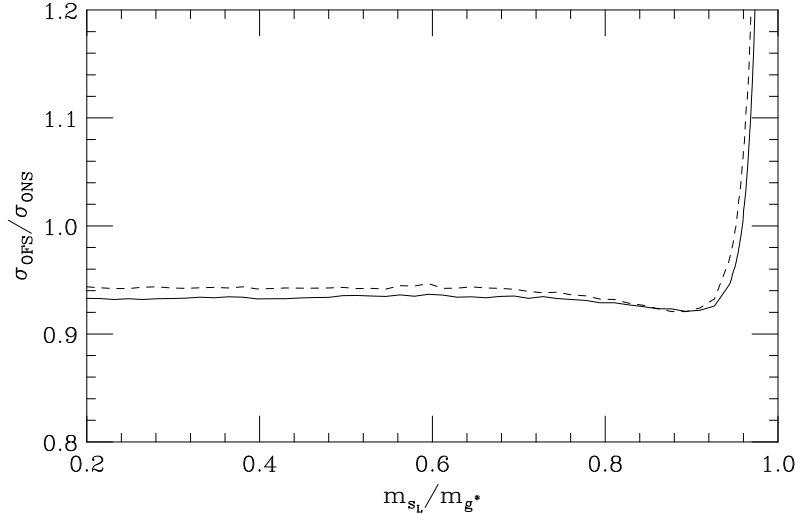


Figure 10: The ratio of the off-shell and on-shell cross section for the process $u \bar{d} \rightarrow \tilde{\chi}_1^+ \tilde{s}_L \bar{s}$ (black line) and its MUED counterpart (dashed line).

simulation there is a choice over which point we should change between using a two- and three-body decay of the particle. If both decays were treated on-shell then the point would simply be the threshold of the two-body decay but when including of off-shell effects for the two-body decay, the choice is not so simple.

Here we use the three-body decay $\tilde{\chi}_2^0 \rightarrow \tilde{\chi}_1^0 e^+ e^-$ in the MSSM to study this effect. The full three-body decay is mediated by a Z^0 boson and both the left- and right-handed selectron, giving an interference between the different channels. If the decay occurs as a series of cascades with a weight factor then these interference effects will be neglected. To judge the extent of the interference we compare the partial width for the decay via the full three-body matrix element and the three-body matrix element with the Z^0 diagram removed and performed as a cascade decay.

Figure 11 shows the results for a range of selectron masses, where both \tilde{e}_L and \tilde{e}_R are degenerate, with $M_{\tilde{\chi}_1^0} = 120.00 \text{ GeV}$ and $M_Z = 91.19 \text{ GeV}$. For a sufficiently large selectron mass there is good agreement between the two methods as there is only a small interference with the Z^0 boson diagram. However, as the mass is lowered so that the decay of the $\tilde{\chi}_2^0$ through the selectron mode becomes closer to being on-shell, the interference effects, particularly just above the Z^0 threshold, become significant and the full three-

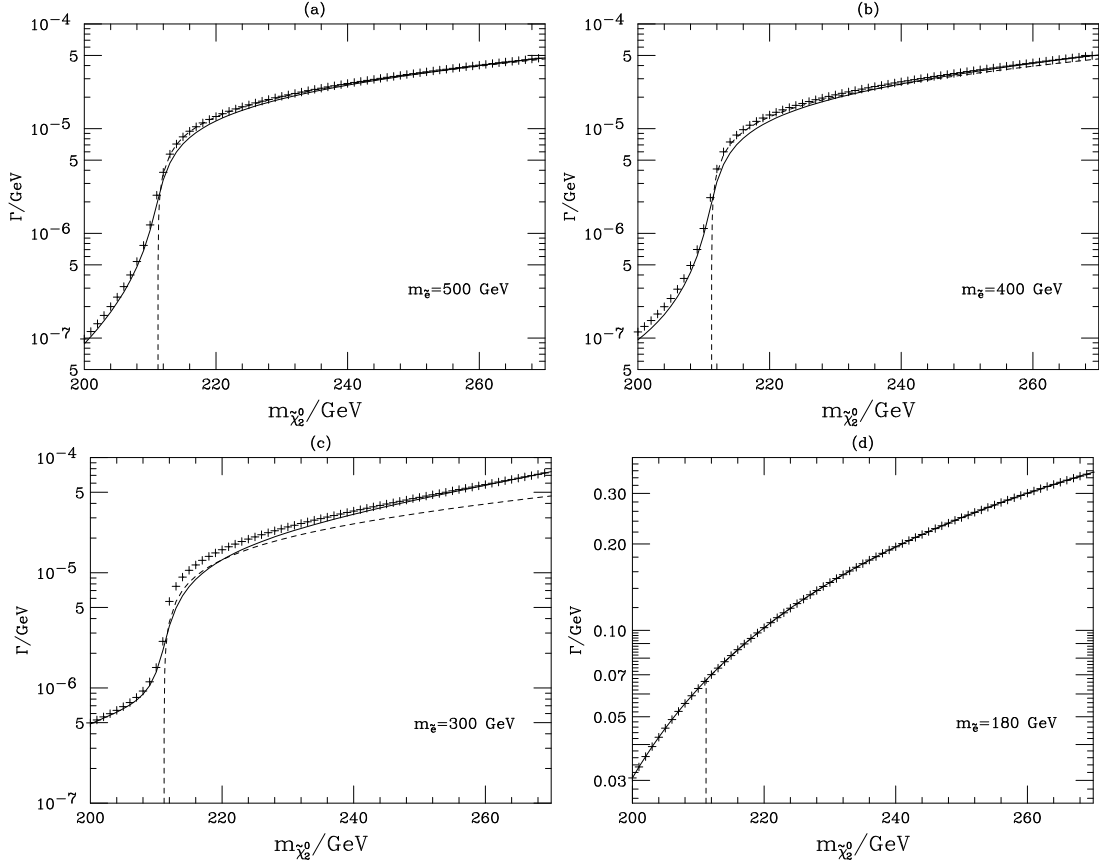


Figure 11: The partial width for the decay $\tilde{\chi}_2^0 \rightarrow \tilde{\chi}_1^0 e^+ e^-$ where the selectron masses are indicated on the plot. The solid line is the full three-body partial width and the crosses are for the three-body decay with the Z^0 diagram removed plus $\Gamma(\tilde{\chi}_2^0 \rightarrow \tilde{\chi}_1^0 Z^0) \times BR(Z^0 \rightarrow e^+ e^-)$. The dashed line shows the two-body on-shell cascade.

body calculation is necessary in this region. For the final case, Fig. 11c, where the selectron modes are on-shell for the whole range there is quite different behaviour. The partial width now smoothly passes over the Z^0 threshold and there is exact agreement with the full three-body result indicating that there is very little or no interference. Given these results it seems reasonable to use the threshold of the on-shell two-body decay as the point where the change from a three-body to a two-body decay with weight factor occurs.

7. Summary

Given that we do not know what type of new physics will be discovered at future colliders, it is necessary to have access to accurate simulations of these new models. An important consideration when studying new physics scenarios within a Monte Carlo event generator is the simulation of off-shell effects. Here we have demonstrated a consistent algorithm for their inclusion in a general-purpose event generator using a variety of processes from the Minimal Supersymmetric Standard and Minimal Universal Extra Dimension Models.

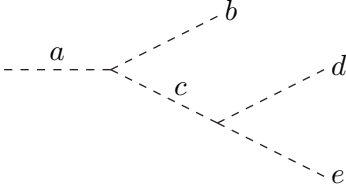


Figure 12: A three-body decay consisting entirely of scalar particles where the external particles a, b, d and e are all on-shell.

The approach described here has been implemented in the `Herwig++` program and will be incorporated in to a future release.

Acknowledgments

We would like to thank our collaborators on the `Herwig++` project and the organisers and participants of the Les Houches 2007 workshop for many useful comments. This work was supported in part by the Science and Technology Facilities Council and the European Union Marie Curie Research Training Network MCnet under contract MRTN-CT-2006-035606.

A. Derivation of Weight Factor

The weight factor introduced in Eq. (3.1) can be derived by considering a three-body decay that consists entirely of scalar particles. Using the notation in Fig. 12, the decay rate is given by

$$\Gamma(a \rightarrow b, d, e) = \frac{(2\pi)^4}{2m_a} \int d\phi_3(p_a; p_b, p_d, p_e) \sum_{i=1}^n \overline{|\mathcal{M}_{3_i}|^2} \quad (\text{A.1})$$

where $d\phi_3$ is the three-body phase-space and $\overline{|\mathcal{M}_3|^2}$ is the spin-averaged matrix element. The phase space can be written recursively as [24, 25]

$$d\phi_3(p_a; p_b, p_d, p_e) = d\phi_2(p_a; p_b, q) d\phi_2(q; p_d, p_e) (2\pi)^3 dq^2, \quad (\text{A.2})$$

where $d\phi_2$ is a two-body phase-space factor and q is the momentum of the intermediate.

For the matrix element assume that the intermediate particle of mass M has n two-body decay modes so that

$$\sum_{i=1}^n \overline{|\mathcal{M}_{3_i}|^2} = \frac{\overline{|\mathcal{M}_a|^2}}{(q^2 - M^2)^2 + q^2\Gamma^2(q)} \sum_{i=1}^n \overline{|\mathcal{M}_{c_i}|^2}, \quad (\text{A.3})$$

where $\overline{|\mathcal{M}_a|^2}$ and $\overline{|\mathcal{M}_{c_i}|^2}$ are the two-body spin-averaged matrix elements and $\Gamma(q)$ is the width of the intermediate at scale q . Substituting Eqns. (A.2,A.3) into Eq. (A.1) gives

$$\Gamma(a \rightarrow b, d, e) = \frac{(2\pi)^3}{m_a} \int dq^2 \frac{q}{(q^2 - M^2)^2 + q^2\Gamma^2(q)} \int d\phi_2 \overline{|\mathcal{M}_a|^2} \int d\phi_2 \frac{(2\pi)^4}{2q} \sum_{i=1}^n \overline{|\mathcal{M}_{c_i}|^2}. \quad (\text{A.4})$$

The third integral in Eq. (A.4) can be recognised as $\Gamma(c \rightarrow d, e)$ using

$$\Gamma(a \rightarrow b, c) = \frac{(2\pi)^4}{2m_a} \int |\overline{\mathcal{M}}_a|^2 d\phi_2 \quad (\text{A.5})$$

and the second as $\Gamma(a \rightarrow b, c)$, with the intermediate at scale q , giving

$$\Gamma(a \rightarrow b, d, e) = \frac{1}{\pi} \int dq^2 \Gamma_a \frac{q\Gamma_c(q)}{(q^2 - M^2)^2 + q^2\Gamma_c^2(q)}. \quad (\text{A.6})$$

The weight factor is then identified as

$$w = \frac{1}{\pi} \int dq^2 \frac{q\Gamma(q)}{(q^2 - M^2)^2 + q^2\Gamma^2(q)}. \quad (\text{A.7})$$

The case for production followed by decay follows similar arguments and the same factor is found.

It should be noted from the discussion in Ref. [20] that use of the running width in the propagator of Eqn. (A.4) is only valid if $\Gamma(q) \sim q$ for large q . If $\Gamma(q)$ were to grow faster than this then the extra terms are dominant and the propagator becomes of $\mathcal{O}(1/\alpha)$, the coupling of the $c \rightarrow d, e$ decay. If $\Gamma(q)$ grows linearly with q the extra terms are just unenhanced higher order corrections.

References

- [1] F. Maltoni and T. Stelzer, *MadEvent: Automatic Event Generation with MadGraph*, *JHEP* **02** (2003) 027, [[hep-ph/0208156](#)].
- [2] A. Pukhov *et. al.*, *CompHEP: A package for evaluation of Feynman diagrams and integration over multi-particle phase space. User's manual for version 33*, [hep-ph/9908288](#).
- [3] A. Pukhov, *CalcHEP 3.2: MSSM, structure functions, event generation, batches, and generation of matrix elements for other packages*, [hep-ph/0412191](#).
- [4] W. Kilian, *WHIZARD 1.0: A generic Monte Carlo integration and Event Generation package for multi-particle processes. Manual*, . LC-TOOL-2001-039.
- [5] M. Moretti, T. Ohl, and J. Reuter, *O'Mega: An Optimizing Matrix Element Generator*, [hep-ph/0102195](#).
- [6] F. Krauss, R. Kuhn, and G. Soff, *AMEGIC++ 1.0: A Matrix Element Generator In C++*, *JHEP* **02** (2002) 044, [[hep-ph/0109036](#)].
- [7] M. Bahr *et. al.*, *Herwig++ Physics and Manual*, 0803.0883.
- [8] G. Corcella *et. al.*, *HERWIG 6: An event generator for hadron emission reactions with interfering gluons (including supersymmetric processes)*, *JHEP* **01** (2001) 010, [[hep-ph/0011363](#)].
- [9] S. Moretti, K. Odagiri, P. Richardson, M. H. Seymour, and B. R. Webber, *Implementation of supersymmetric processes in the HERWIG event generator*, *JHEP* **04** (2002) 028, [[hep-ph/0204123](#)].

- [10] T. Sjostrand, S. Mrenna, and P. Skands, *PYTHIA 6.4 Physics and Manual*, *JHEP* **05** (2006) 026, [[hep-ph/0603175](#)].
- [11] T. Sjostrand, S. Mrenna, and P. Skands, *A Brief Introduction to PYTHIA 8.1*, [arXiv:0710.3820](#).
- [12] T. Gleisberg *et. al.*, *SHERPA 1.α, A Proof-of-Concept Version*, *JHEP* **02** (2004) 056, [[hep-ph/0311263](#)].
- [13] I. G. Knowles, *Spin Correlations in Parton-Parton Scattering*, *Nucl. Phys.* **B310** (1988) 571.
- [14] J. C. Collins, *Spin Correlations in Monte Carlo Event Generators*, *Nucl. Phys.* **B304** (1988) 794.
- [15] P. Richardson, *Spin Correlations in Monte Carlo Simulations*, *JHEP* **11** (2001) 029, [[hep-ph/0110108](#)].
- [16] M. Gigg and P. Richardson, *Simulation of Beyond Standard Model Physics in Herwig++*, *Eur. Phys. J.* **C51** (2007) 989–1008, [[hep-ph/0703199](#)].
- [17] D. Berdine, N. Kauer, and D. Rainwater, *Breakdown of the Narrow Width Approximation for New Physics*, *Phys. Rev. Lett.* **99** (2007) 111601, [[hep-ph/0703058](#)].
- [18] N. Kauer, *Narrow-Width Approximation Limitations*, *Phys. Lett.* **B649** (2007) 413–416, [[hep-ph/0703077](#)].
- [19] N. Kauer, *A Threshold-Improved Narrow-Width Approximation for BSM physics*, [0708.1161](#).
- [20] M. H. Seymour, *The Higgs Boson Line Shape and Perturbative Unitarity*, *Phys. Lett.* **B354** (1995) 409–414, [[hep-ph/9505211](#)].
- [21] W. Beenakker *et. al.*, *WW Cross-sections and Distributions*, [hep-ph/9602351](#).
- [22] B. C. Allanach *et. al.*, *The Snowmass Points and Slopes: Benchmarks for SUSY Searches*, [hep-ph/0202233](#).
- [23] W. Porod, *SPheno, A program for calculating supersymmetric spectra, SUSY particle decays and SUSY particle production at e+ e- colliders*, *Comput. Phys. Commun.* **153** (2003) 275–315, [[hep-ph/0301101](#)].
- [24] **Particle Data Group** Collaboration, W. M. Yao *et. al.*, *Review of Particle Physics*, *J. Phys.* **G33** (2006) 1–1232.
- [25] J. D. Jackson, *Remarks on the phenomenological analysis of resonances*, *Nuovo Cim.* **34** (1964) 1644–1666.